TRANSACTIONS OF THE INSTITUTE OF AVIATION
No. 2 (239), pp. 53-71, Warsaw 2015

eISSN 2300-5408

FLIGHT ENVELOPE OF LIGHT HELICOPTER WITH ADDITIONAL PROPULSION PROPELLER

Jarosław Stanisławski

New Technology Center, Aircraft Design Department, Institute of Aviation, al. Krakowska 110/114, 02-256 Warsaw, Poland, jaroslaw.stanislawski@ilot.edu.pl

Abstract

The paper presents possibilities of changing a flight envelope of a light helicopter with an additional propeller. Using the propulsion propeller enables to reduce the power required for the main rotor driving in high speed flight conditions. The results of simulating calculations for the conventional helicopter and for the version with the additional propeller are compared. For calculations of the equilibrium flight conditions of the helicopter is used the simple model consisting of a point mass fuselage and a rotor treated as a disk. The more detailed model of the elastic blade is applied to compute the level of rotor loads and blades deformations. The equations of motion of deformable blade are solved by applying Runge-Kutta method.

Keywords: helicopter, pushing propeller, rotor.

1. INTRODUCTION

In recent years a tendency is observed to increase flight speeds of the helicopter by applying additional devices generating enlarged amount of thrust necessary to balance the forces of the aerodynamic drag. The related reduction of a horizontal component of the main rotor thrust may also iwwnfluence the delay of the adverse effects of compressibility and the rise of the rotor power. As new constructions of the compound helicopters with the additional propulsion can be mentioned [1]: the Piasecki X-49 Speed Hawk, experimental the Sikorsky X-2, military the Sikorsky S-97 Raider and French Eurocopter X3. The Piasecki X-49 is based on the airframe of transport helicopter UH-60 Black Hawk with built-in additional wings and vectored thrust ducted propeller in the tail of the fuselage. The experimental Sikorsky X-2 and now being developed the X-97 Raider [2], [4] are built with an application of two coaxial rotors system with the additional pushing propeller mounted in the tail of the fuselage. In September 2010 the X-2 helicopter reached the speed of 250knots in level flight exceeding the world top speed record of 216knots (400km/h) for helicopter set in 1986 by the Westland Lynx with BERP rotor [5]. The French hybrid helicopter the Eurocopter X3 is based on fuselage of the EC 155 with the five-bladed main rotor system and the additional short span wings each fitted with the tractor propeller. The distance between the axes of the propellers and a possibility of generating thrust at the opposite directions allows to remove the tail rotor. On June 7, 2013 the Eurocopter X3

set a new record for the helicopter achieving in level flight the speed of 255knots (472km/h). The recent research activity of Polish Institute of Aviation (Warsaw) includes the development of helicopter technology comprising the range of lower flight speed [6], [7].

The paper presents results of calculation concerning an influence of mounting the additional propulsive propeller on changes the flight states attainable for a light helicopter with the articulated three-bladed main rotor and with the tail rotor. The scheme of the helicopter arrangement including the main rotor, the tail rotor and the additional propeller in the tail of the fuselage is shown in Fig. 1. The considered systems of rotors and the propeller with the preserved tail rotor is similar to the composition of the Lockheed AH56 Cheyenne attack helicopter tested in the sixties.

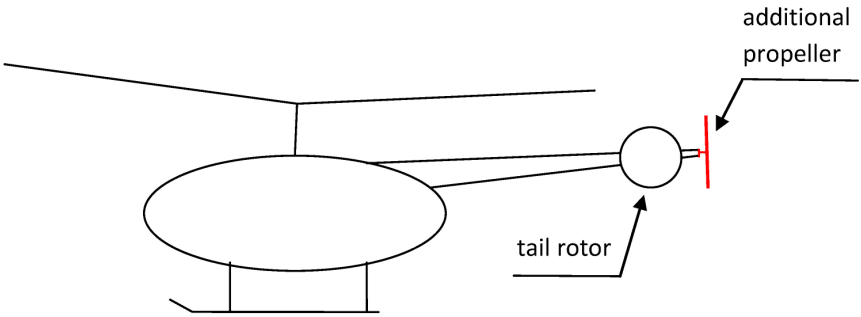

Fig. 1. Scheme of helicopter with the additional propulsive propeller. [Author, 2015]

An influence of the additional propeller on a helicopter's balance and the level of the required power due to the flight speed was defined based on calculation results of a computer program [8] applying a simplified model of the point-mass fuselage and the main rotor treated as the disk area. The initially determined equilibrium conditions of the helicopter next are used as a part of the input data for the program calculating the rotor loads. The simulation program applies a more precise model of an elastic blade[9]. Equations of motion of the deformable rotor blade are solved by means of the Runge-Kutta method including the effects of blade bending deflections, torsion and control of collective and cyclic pitch.

2. COMPARISON OF HELICOPTER FLIGHT CONDITIONS

The calculations of the equilibrium flight conditions and the required power as a function of speed flight were performed for two variants of helicopter configurations: conventional and the rotorcraft with additional pushing propeller and the preserved tail rotor. For both variants of the helicopter the take-off mass of 1,100kg is assumed. The basic data of the main rotor, the tail rotor and the additional propeller are collected in Table 1.

Table 1. Basic data of rotors and propeller.

	number of blades	radius [m]	blade tip speed [m/s]	blade chord [m]
main rotor	3	3.75	186	0.20
tail rotor	5	0.432	177	0.10
propeller	4	0.75	195	0.15

Applying the additional propeller enables to generate a level thrust which allows to reduce a horizontal component of the main rotor thrust by a lesser pitch of the swashplate and a pitch angle of fuselage. In the calculation program of the equilibrium flight states of the helicopter with the additional propeller it was assumed that the propeller thrust is equal to the aerodynamic drag of the helicopter. The comparison of the power required for a flight for two versions of the helicopter is shown in Fig. 2. It can be noticed that at higher speed range over 200km/h, the total required power takes lower values for the compound version with the propeller. In Fig. 2 is shown the plot of the assumed power unit level, which provides reaching the maximum speed of flight higher by about 10km/h for the compound helicopter with the propeller in comparison with the conventional helicopter. In the range of the flight speed lower than 180km/h the conventional helicopter takes advantage of the lesser value of the total power required for a flight. In Fig. 3 ÷ Fig. 5 are compared the values of the required power in separation for the main rotor, the tail rotor and the additional propeller. Respectively, the plots of the thrust are presented in Fig. 6 for the main rotor, in Fig. 7 for the tail rotor and in Fig. 8 for the propeller. The differences of values of the required power and the generated thrust largely depend on the pitch angle for the same flight speed (Fig. 9). The sharp changes of plots in Fig.6, 9, 12 observed below speed of 70 km/h are connected with transition of the separation airflow at horizontal stabilizer, which affects the equilibrium state of helicopter. Applying the additional propeller enables a significant reduction of the horizontal component of the main rotor thrust providing the equilibrium of the helicopter at the range of the higher flight speed (Fig. 10). The additional factor, which reduces the aerodynamic drag, is the lower pitch angle of the fuselage equals 1^0 in flight at the speed of 200km/h for the rotorcraft with the propeller in

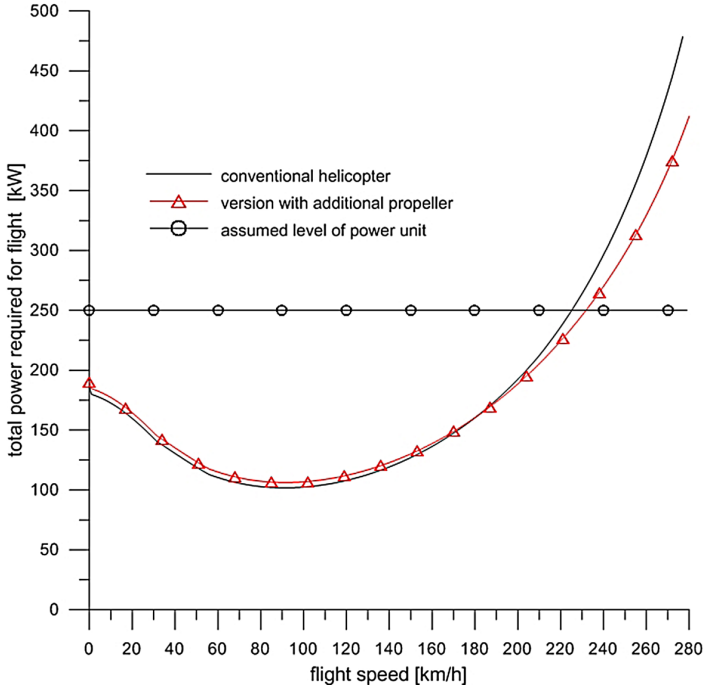

Fig. 2. Power required for flight of helicopter, effect of the additional propulsive propeller, helicopter mass 1,100kg. The case of the three-bladed main rotor and the four-bladed push propeller. [Author, 2015]

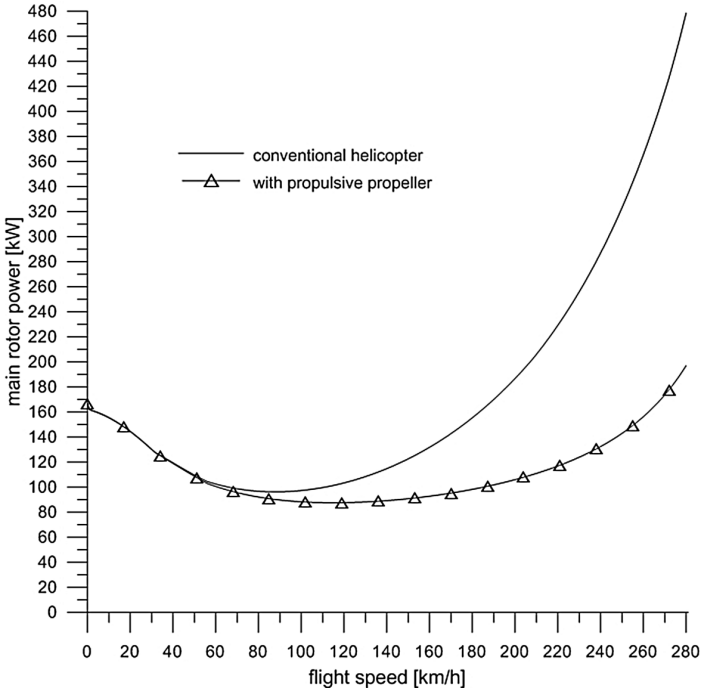

Fig. 3. Power required to drive the main rotor as function of the flight speed, effect of applying the propulsive propeller, helicopter mass 1,100kg. The case of the three-bladed main rotor and the four-blade additional propeller. [Author, 2015]

comparison with nearly 7^0 of fuselage pitch for the conventional helicopter. The reduced level of the main rotor required power for the variant with the pushing propeller (Fig. 3) also means the diminished demands for the thrust (Fig. 7) and power (Fig. 4) of the tail rotor. The demanded thrust and the required power for driving the propeller rises with the flight speed but it must be noticed that in the range of the higher speed the growth of the additional propeller power is lower than the growth of the main and tail rotors' common power for the conventional helicopter variant. In the higher speed range the additional propeller requires a considerable power in comparison with the main rotor power. At the speed of 200km/h the propeller power equals 80kW, while the main rotor power equals 106kW. In equilibrium conditions in the range of a low speed of flight the additional propeller power is definitely lower, not exceeding the value of 20kW up to the speed of 118km/h. An increased level of the propeller power can be foreseen in a maneuver when the enlarged thrust of the propeller can be used for helicopter acceleration or deceleration without the change of fuselage pitch angle.

The changes of power and thrust due to the flight speed increase are related with the position of the control system elements:

- collective pitch of the main rotor blades (Fig. 11),
- deflection angles of swashplate (Fig. 12 and Fig. 13),
- pitch angle of the tail rotor blades (Fig.14),
- propeller blades pitch angle (Fig.15).

Comparing two variants of the helicopter in the higher speed range the significant difference is noticed between the pitch angles of the tail rotor blades, which is connected with the lesser value of the main rotor power for the compound version with the propeller.

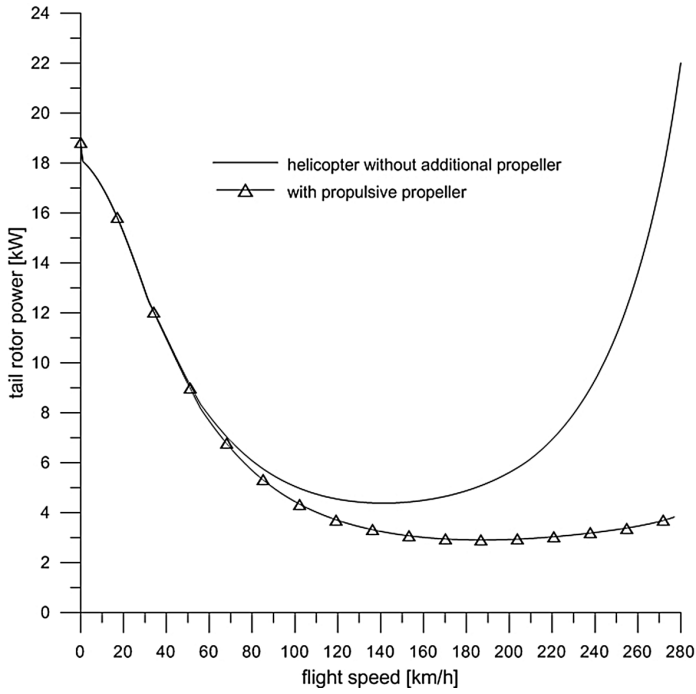

Fig. 4. Power required to drive the tail rotor due to flight speed, for two helicopter configurations: conventional and with the additional propulsive propeller; helicopter mass 1,100kg. [Author, 2015]

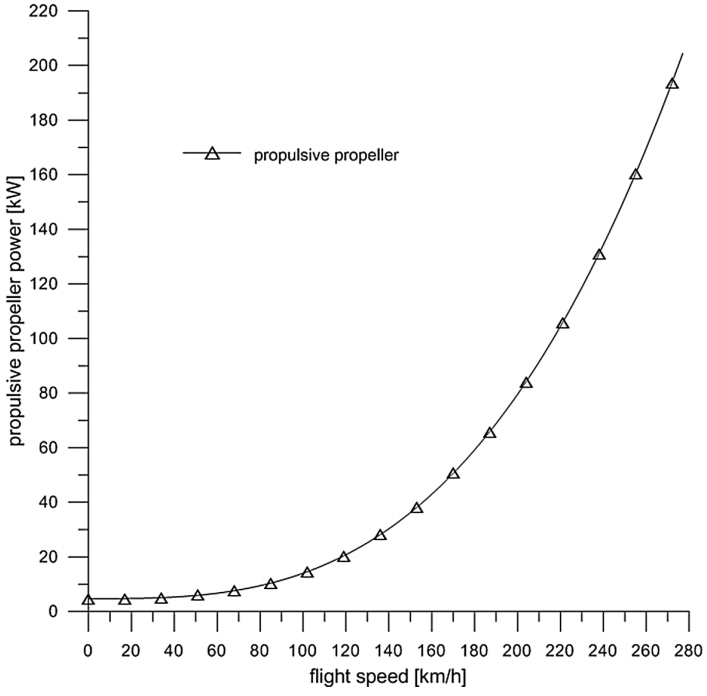

Fig. 5. Power required for driving the propulsive propeller due to flight speed; helicopter mass 1,100kg, the four-bladed propeller. [Author, 2015]

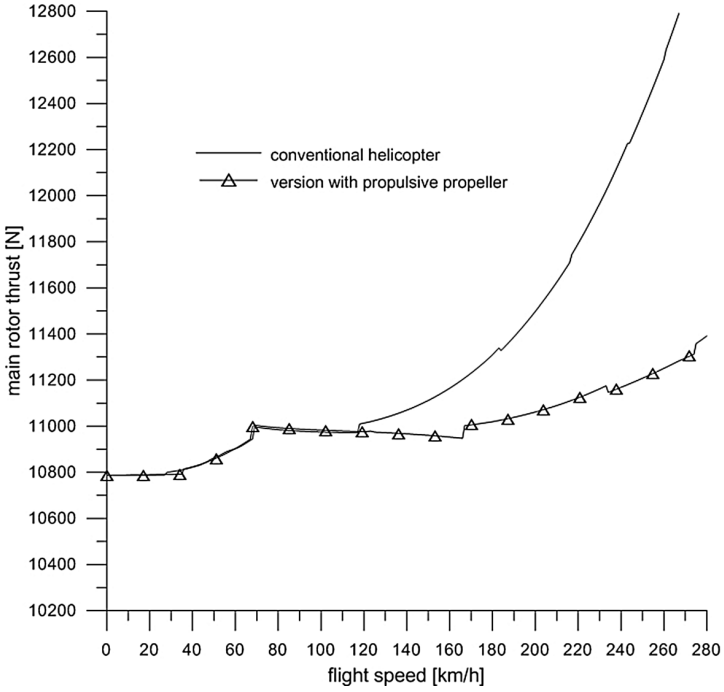

Fig. 6. Comparison of the main rotor thrust, as a function of the flight speed, for the two versions of helicopter: conventional and with the additional propeller; helicopter mass 1,100kg. [Author, 2015]

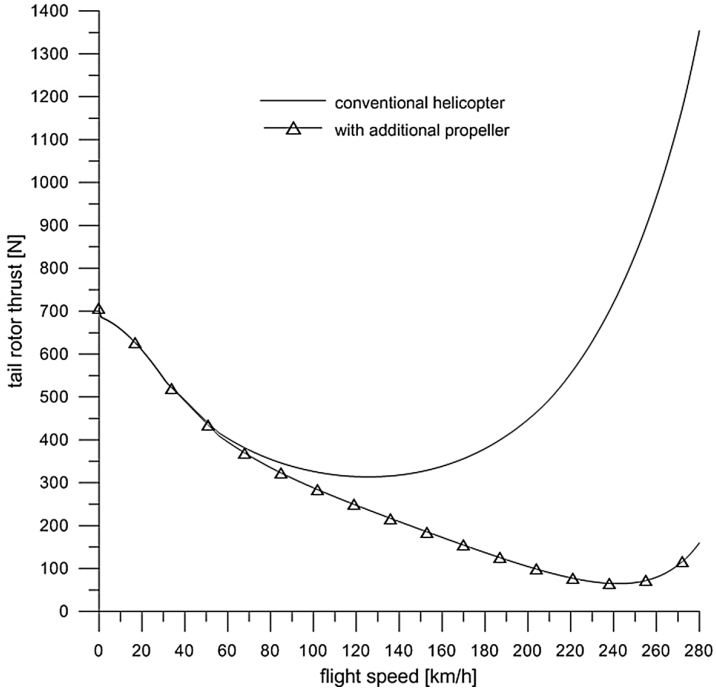

Fig. 7. Tail rotor thrust due to flight speed for the two versions of helicopter; helicopter mass 1,100kg. [Author, 2015]

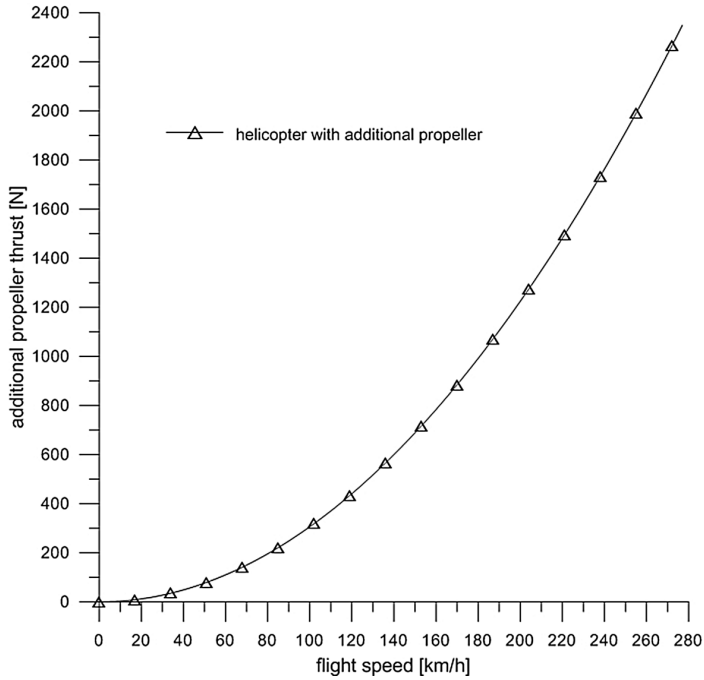

Fig. 8. Thrust of the propulsive propeller required for the level flight conditions; helicopter mass 1,100kg. [Author, 2015]

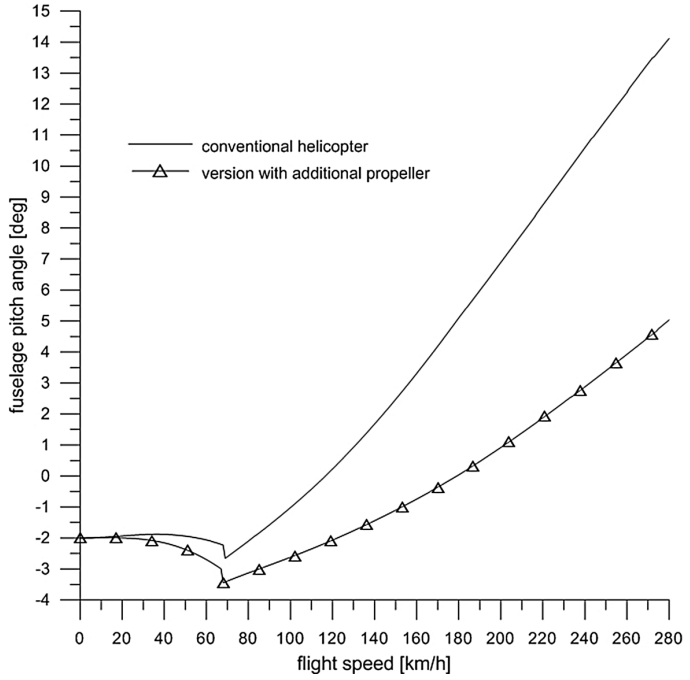

Fig. 9. Changes of the fuselage pitch angle in the level flight conditions for two versions of helicopter configuration: conventional and with the propulsive propeller; helicopter mass 1,100kg, (+) for fuselage nose down. [Author, 2015]

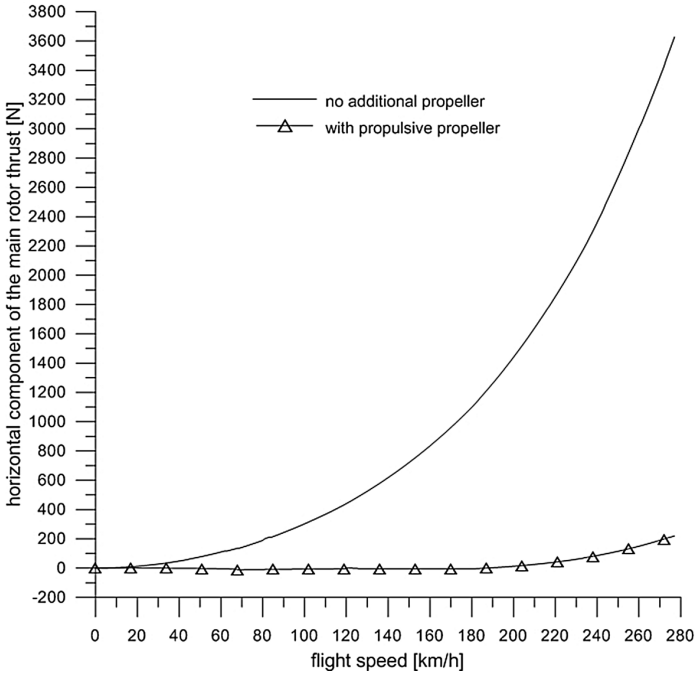

Fig. 10. Changes of the horizontal component of the main rotor thrust in the level flight conditions for two versions of helicopter configuration: conventional and with the propulsive propeller; helicopter mass 1,100kg. [Author, 2015]

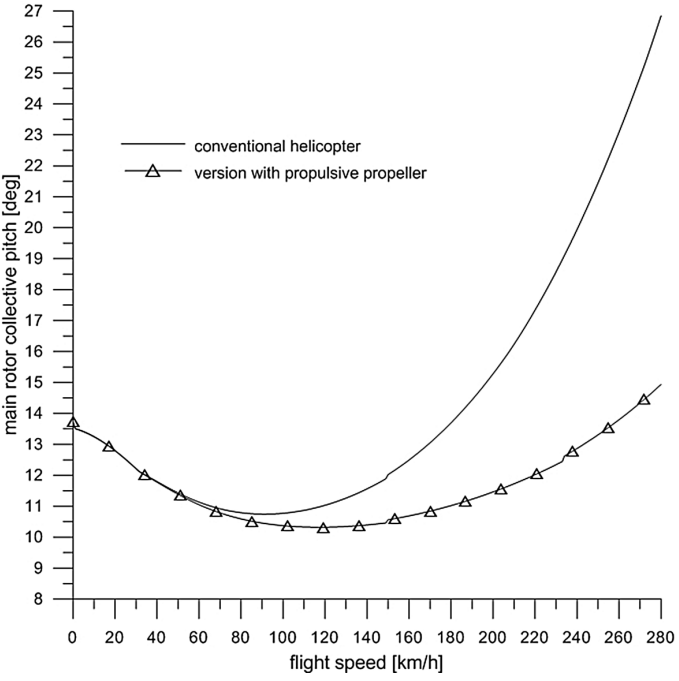

Fig. 11. Changes of the collective pitch of the main rotor blades at 0.7 radius in the level flight conditions for two versions of helicopter configuration: conventional and with the propulsive propeller; helicopter mass 1,100kg. [Author, 2015]

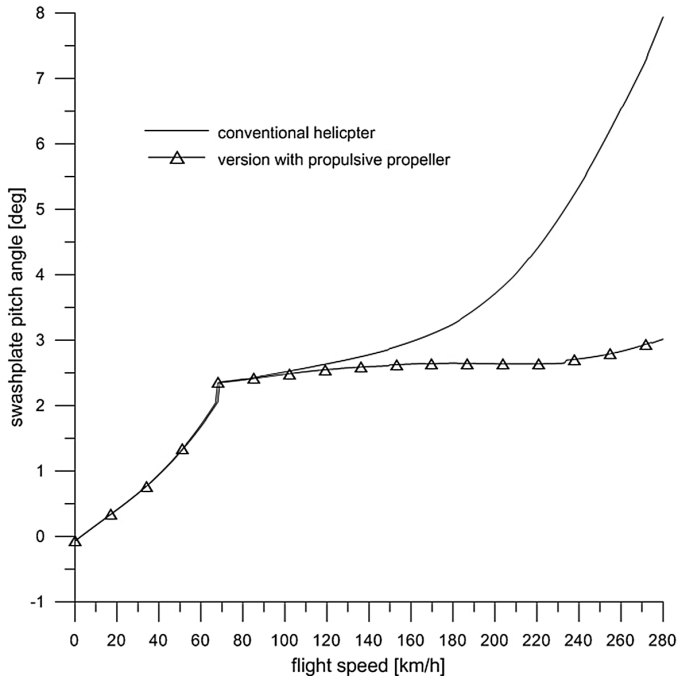

Fig. 12. Changes of the pitch angle of the swashplate in the level flight conditions for two versions of helicopter configuration: conventional and with the propulsive propeller; helicopter mass 1,100kg, (+) for the stick push-over [Author, 2015]

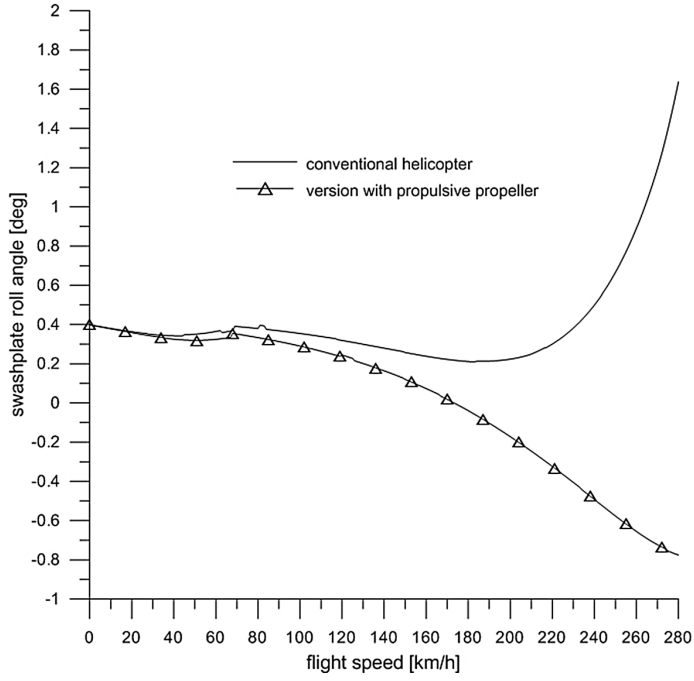

Fig. 13. Changes of the roll angle of the swashplate in the level flight conditions for two versions of helicopter configuration: conventional and with the propulsive propeller; helicopter mass 1,100kg, (+) for the stick toward azimuth of 270^0 [Author, 2015]

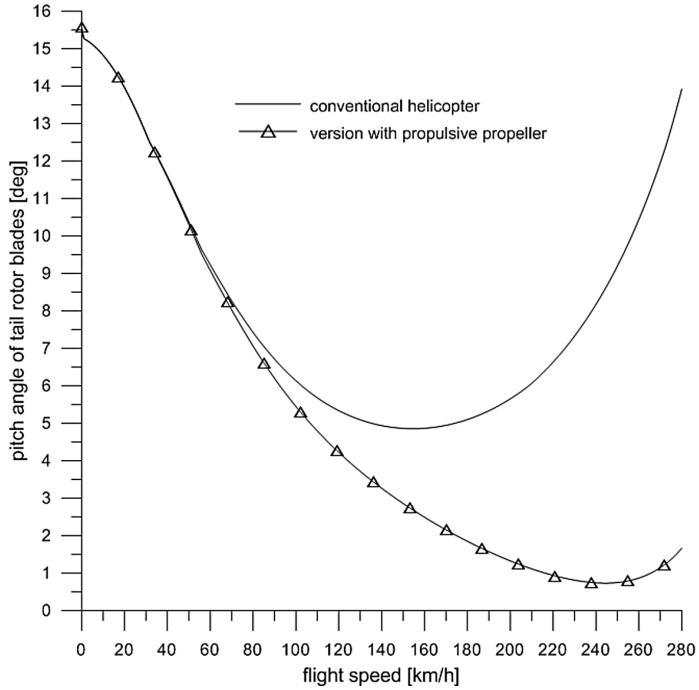

Fig. 14. Changes of the pitch angle of the tail rotor blades in the level flight conditions for two versions of helicopter configuration: conventional and with the propulsive propeller; helicopter mass 1,100kg. [Author, 2015]

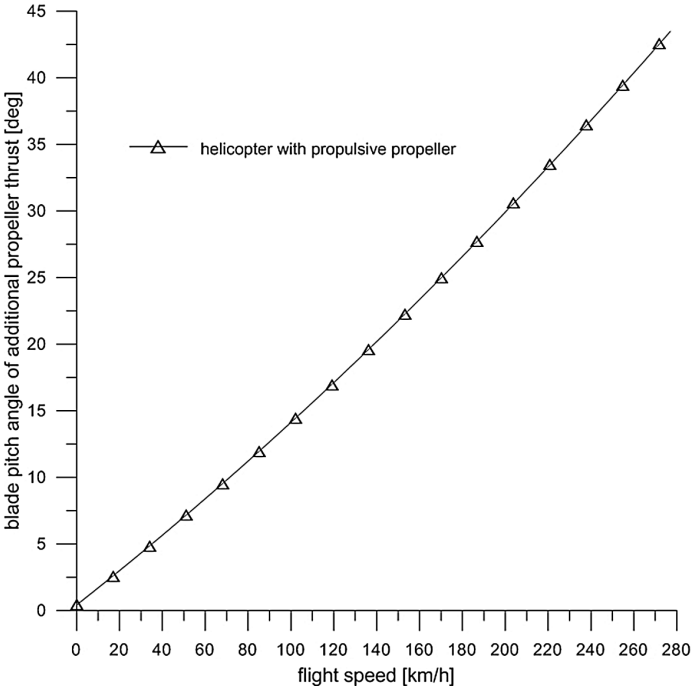

Fig. 15. Changes of the blade pitch angle of the propulsive propeller at 0.7 radius due to flight speed, helicopter mass 1,100kg [Author, 2015]

3. CHANGES OF ROTOR LOADS AND BLADE DEFORMATIONS

The defined equilibrium conditions of the helicopter flight were used as input data for a calculation of the blade deformations and the rotor loads for both versions of the helicopter. For comparison the data for level flight at the speed of 200km/h conditions were applied. The results of the calculations are presented in the form of time-run plots for the following parameters:

- components of the main rotor loads: power (Fig. 16) and thrust (Fig. 17),
- deformations of the main rotor blade (Fig. 18 and Fig. 19),
- angle of attack at the tip section of the rotor blade (Fig. 20),
- position of elements of the main rotor control system (Fig. 21-Fig. 23)

In Fig. 24 and Fig. 25 are presented on the rotor disk the distributions of the differences between a critical attack angle (a separation flow) and a local angle of attack. In Fig. 27 are shown the time-runs of the main rotor thrust of the compound helicopter for the different flight speed compared to the time-run of the main rotor thrust for the conventional variant at the speed of 200km/h. In Fig. 26 and Fig. 28 are presented the distributions of differences of the critical and local angles of attack for the main rotor of the compound helicopter with the propeller at the speed of 240km/h and 280km/h respectively.

The simulation calculations of the rotor loads were performed for an interval of time corresponding the twelve revolutions of the main rotor shaft. The plots show the time-runs for the last two rotor revolutions. In the case of differences of the attack angles the plots show its distributions for the 10^{th} revolution of rotor.

The calculated time-runs of the main rotor power (Fig. 16) and thrust (Fig. 17) show a lower level of the required power and thrust in flight at the speed of 200km/h for the version of the helicopter with the additional propeller. The plots present the three cycles of load changes per rotor revolution which is characteristic for the three-bladed rotors. The reduced loads of the main rotor are generated by the sum of reactions of all three blades. However, for the single blade at the tip section are observed slightly increased torsion (Fig. 18) and bending (Fig. 19) deformations. For the compound helicopter the local increase out-of-plane deflections at tip of the rotor blade in the vicinity of 180^{o} azimuth observed in Fig.19 is connected with the different fuselage pitch angle (Fig.9) at the equilibrium flight conditions at speed of 200km/h for compound and conventional version of helicopter. In the case of the helicopter with the pushing propeller at flight with nearly horizontal position of the main rotor in-plane in the vicinity of 180^{o} azimuth appears the zone of airflow across the rotor disk from below to above it, in the opposite direction of the rotor induced velocity, which increases the local attack angles at root and middle sections of the rotor blade. Such effect can be noticed comparing the distribution plots of difference of critical and local attack angles for root and middle sections of blade at 180^{o} azimuth for the conventional and compound helicopter (Fig.24, Fig.25). For both versions of the helicopter the plots of the angle of attack for the blade tip section are similar but for the compound helicopter in vicinity of the azimuth 270^{O} for the retreating blade occurs a zone of lesser attack angles (Fig. 20). The differences of airflow of rotor blade sections at the same flight speed for two versions of the helicopter clearly appear in plots of the loads of the rotor control system elements. For the helicopter version with the propeller the pitch control moment of the rotor blade reaches the lower values at the larger part of azimuth positions compared with the blade control moment of the conventional helicopter (Fig. 21). Flight at the same speed, but with the different pitch angle of the rotor shaft and collective pitch of rotor blades, gives the different time-runs of the swashplate pitch moment (Fig. 22) and control force of the blade collective pitch (Fig. 23). In the case of the swashplate pitch moment a comparable value but opposite sense for two variants of the helicopter can be related to the light pulled-up stick position and the lesser pitch of the rotor plane in the level flight for compound helicopter comparing with the conventional one.

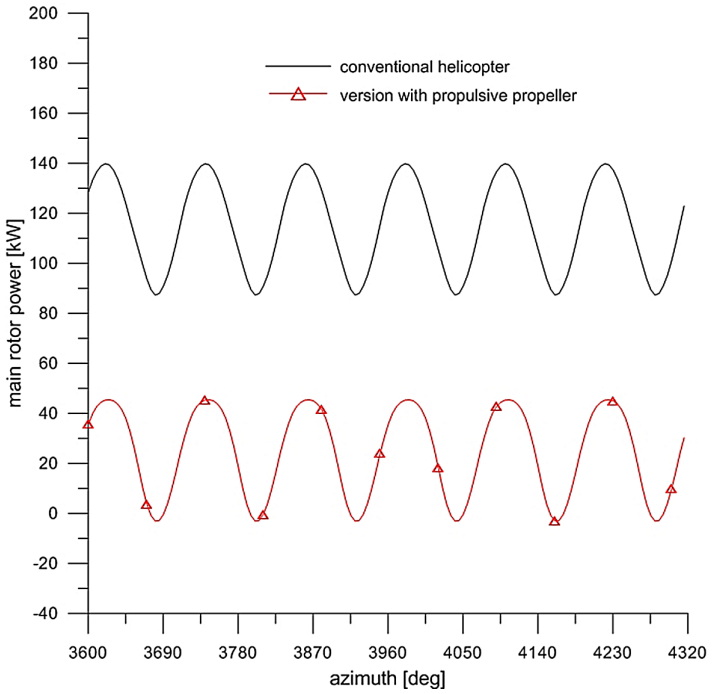

Fig. 16. Time-run of the main rotor power in level flight condition at speed V=200km/h for two versions of helicopter configurations: conventional and with the propulsive propeller. [Author, 2015]

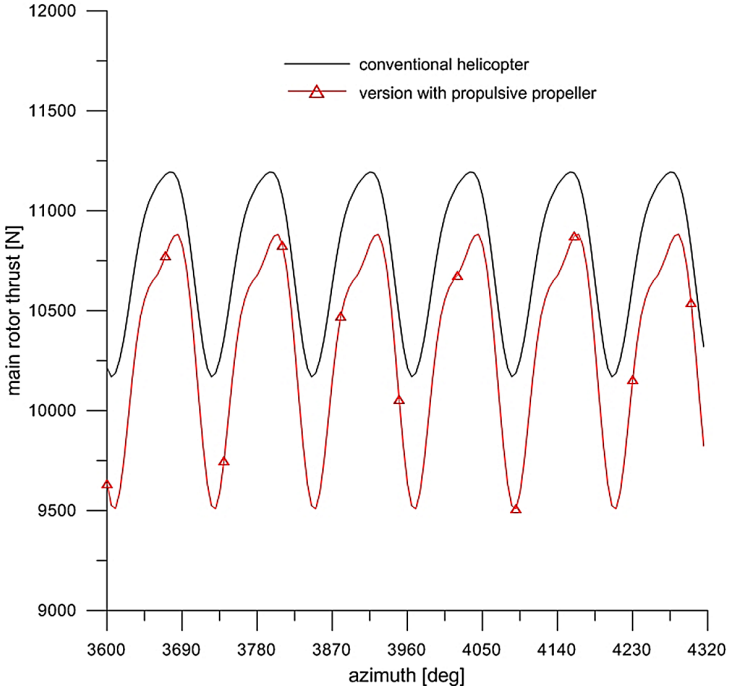

Fig. 17. Main rotor thrust in level flight condition at speed V=200km/h, for two versions of helicopter configurations: conventional and with the propulsive propeller. [Author, 2015]

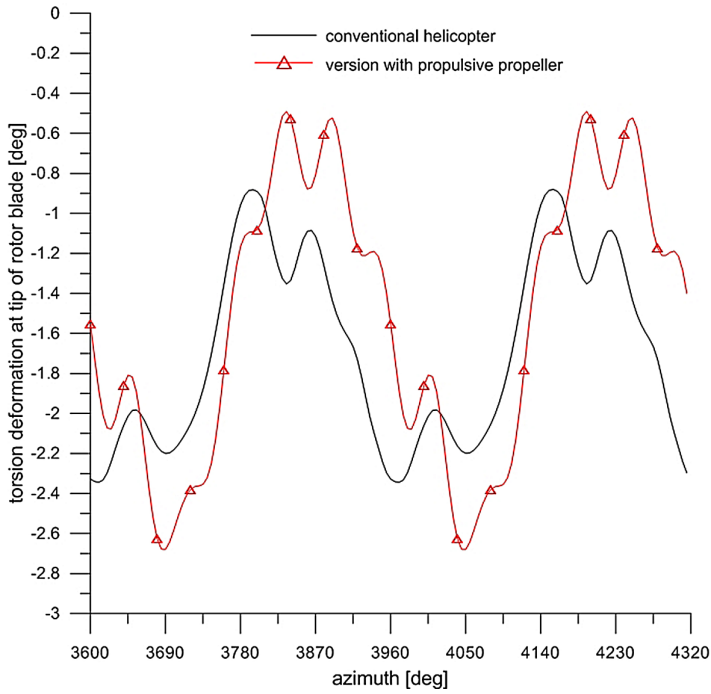

Fig. 18. Torsion deformation at tip of the main rotor blade in level flight conditions at speed V=200km/h for the conventional helicopter and configuration with the propulsive propeller.
A simulation solution for two revolutions of the main rotor. [Author, 2015].

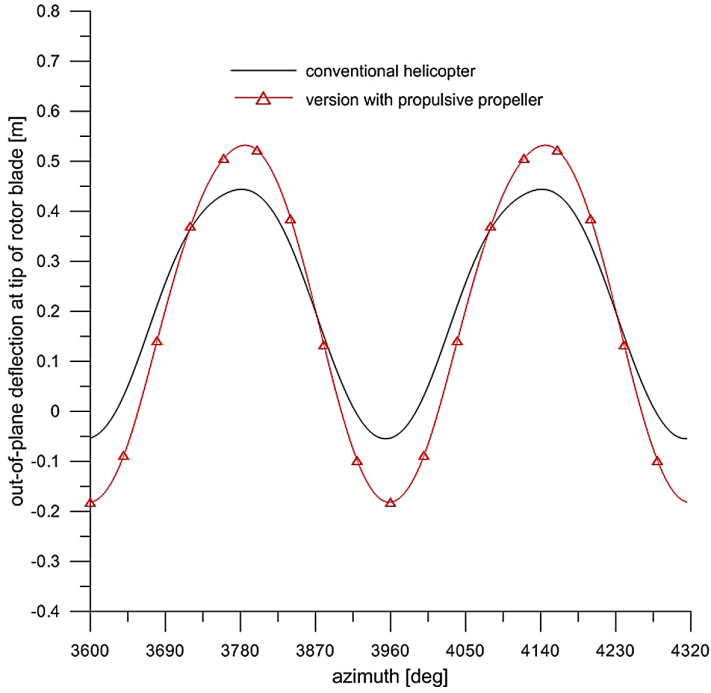

Fig. 19. Out-of-plane deflection at tip of the main rotor blade in level flight conditions at speed V=200km/h for the conventional helicopter and configuration with the propulsive propeller. [Author, 2015].

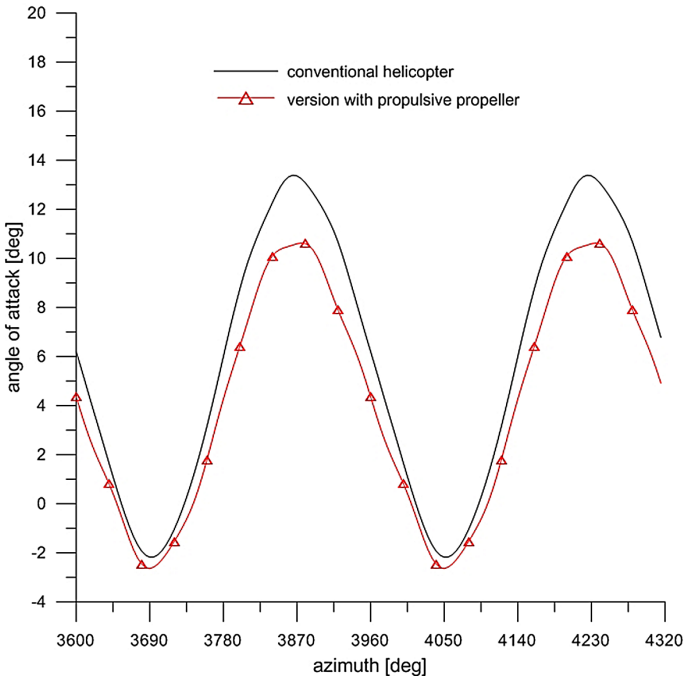

Fig. 20. Angle of attack at tip of the main rotor blade due to azimuth position in level flight conditions at speed V=200km/h for the conventional helicopter and configuration with the propulsive propeller. [Author, 2015].

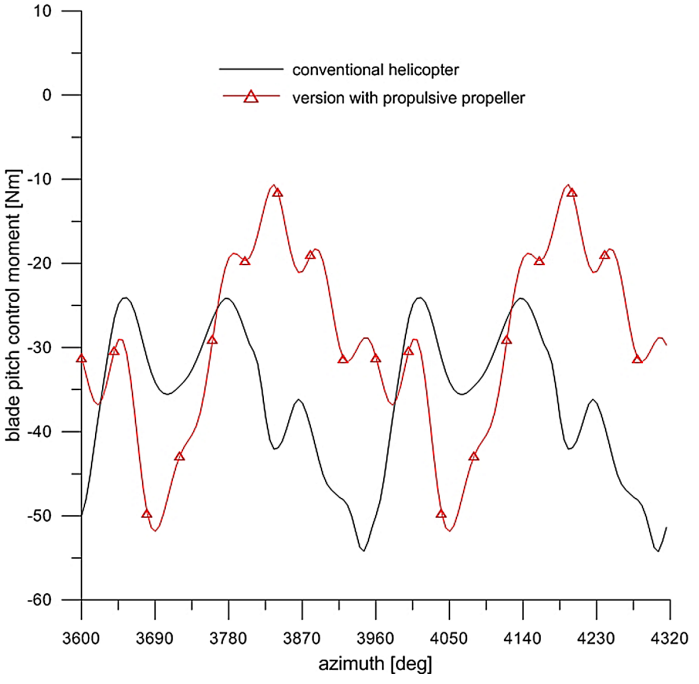

Fig. 21. Changes of pitch control moment of main rotor blade due to azimuth position in level flight conditions at speed V=200km/h. The comparison for the conventional helicopter, and configuration with the propulsive propeller; helicopter mass 1,100kg. [Author, 2015]

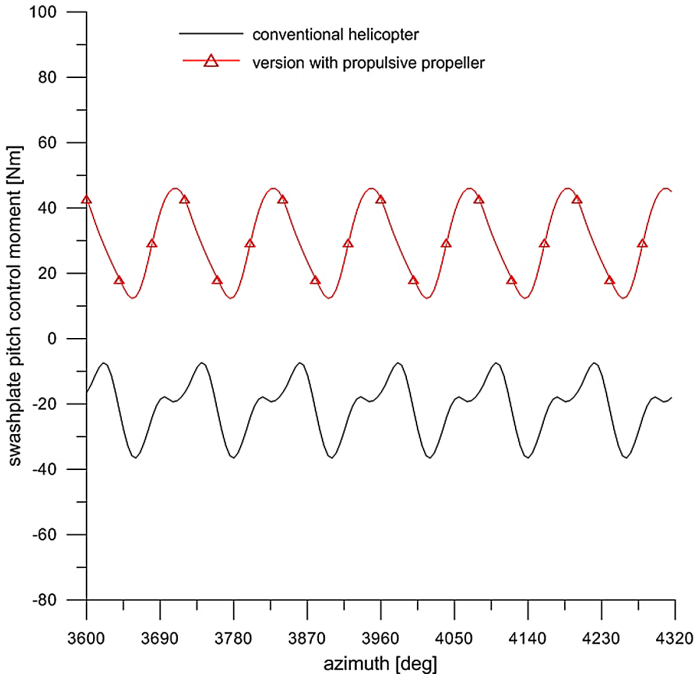

Fig. 22. Changes of pitch control moment of swashplate as a function of azimuth position in level flight conditions at speed V=200km/h. The comparison for the conventional helicopter, and configuration with the propulsive propeller; helicopter mass 1,100kg. [Author, 2015]

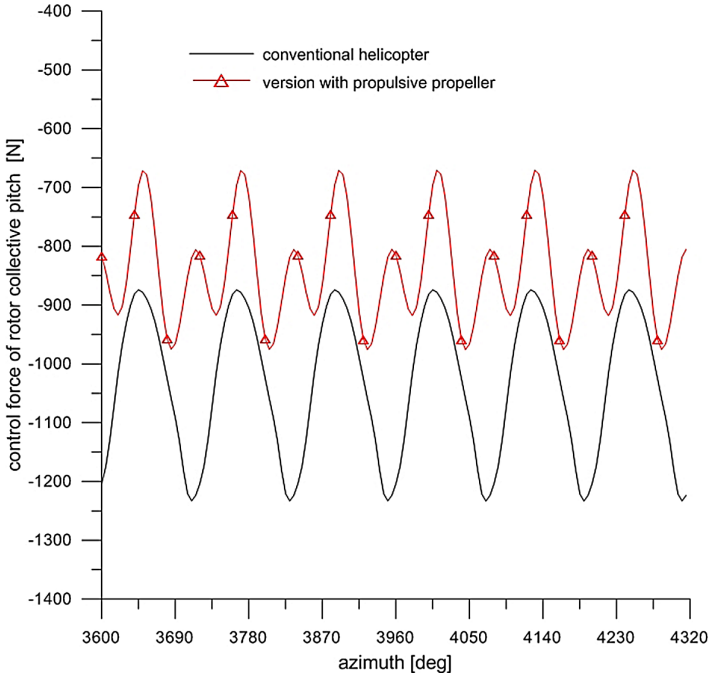

Fig. 23. Control force of collective pitch of all main rotor blades in level flight conditions at speed V=200km/h. The comparison for the conventional helicopter, and configuration with the propulsive propeller; helicopter mass 1,100kg. [Author, 2015]

The differences of critical and local attack angles are presented as plots of distributions on the rotor disk. The negative values of differences show the zones of separation airflow. The izoline of zero value indicates the boundary of the separation flow area. Comparing the distributions of differences of the attack angles for the conventional helicopter (Fig. 24) and for the compound one with the propeller (Fig.25), it can be noticed in the case of the compound helicopter the large margin to the separation limit for the blade tip sections at the azimuth of 270^0 position and appearance the separation airflow zone for the blade sections between azimuth of 180^0-270^0 at root and at the middle of radius. The results of simulations for the higher flight speed of 240km/h (Fig. 26) and 280km/h (Fig. 28) show the fast increase of the zone of a separation airflow, which leads to enlarging the amplitude of the main rotor thrust and generating the adverse vibrations of the whole stricture of the helicopter. For the compound helicopter the separation zone location and increase of its area due to flight speed are connected with relatively smaller pitch angle of fuselage at the equilibrium flight conditions (Fig.9) in comparison with the compound helicopter. The small pitch angle of the main rotor shaft axis in the case of the compound helicopter causes the enlarged airflow across the rotor disk directed above it, which is similar to early transition phase of autorotation state or pull-up maneuver . At such flow conditions the separation zone appears in vicinity of root and middle sections of the blade. Increase of separation zone on the rotor disk can be partly limited by optimization of fuselage pitch due to change of rotor cyclic pitch or change the incidence angle of horizontal tail plane. Application the additional stub wings may also diminish the separation zone on the rotor disk.

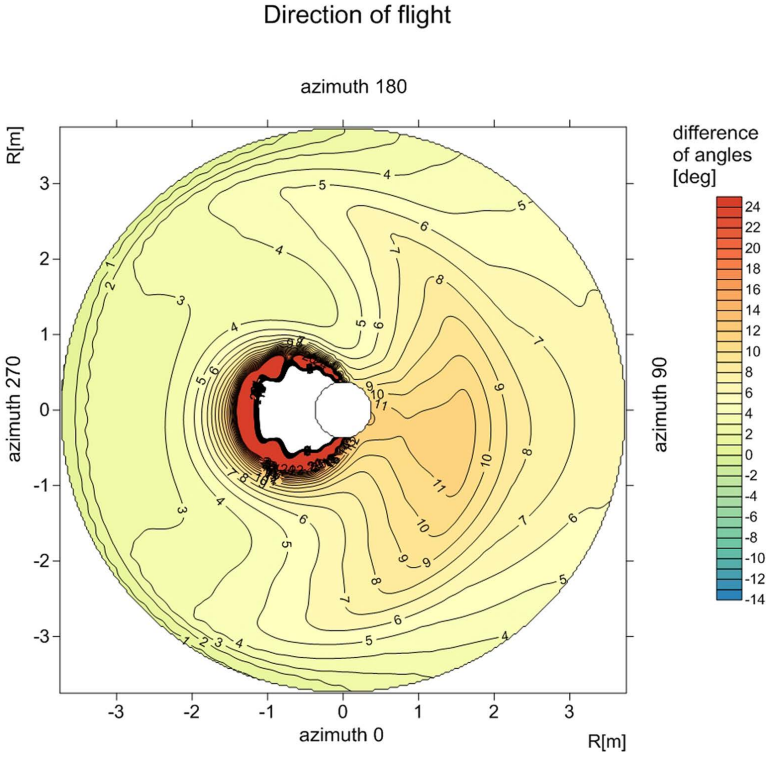

Fig. 24. Main rotor disk distribution of difference of critical and local attack angles of blade cross-sections in level flight at speed 200km/h. The case for conventional helicopter. [Author, 2015]

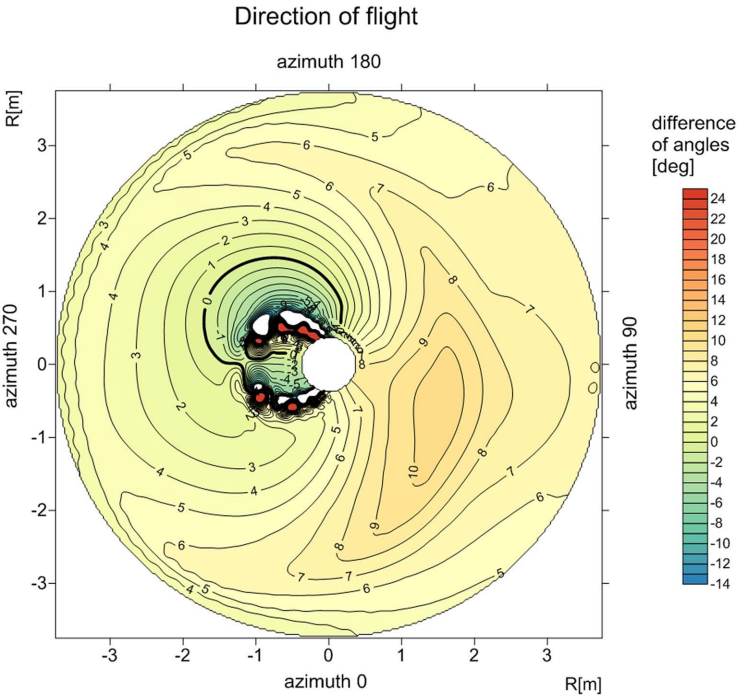

Fig. 25. Main rotor disk distribution of difference of critical and local attack angles of blade cross-sections in level flight at speed 200km/h.
The case for the helicopter with propulsive propeller. [Author, 2015]

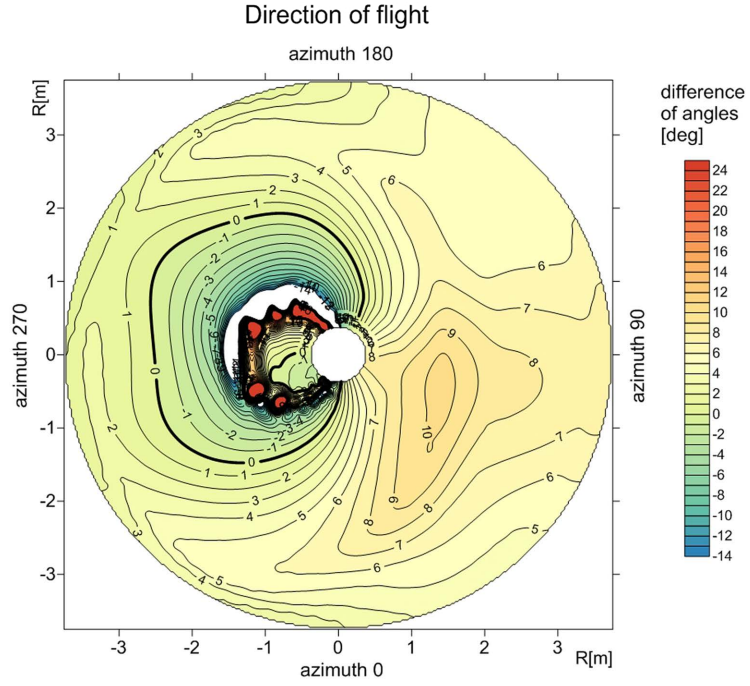

Fig. 26. Main rotor disk distribution of difference of critical and local attack angles of blade cross-sections in level flight at speed 240km/h. The case for the helicopter with propulsive propeller. [Author, 2015]

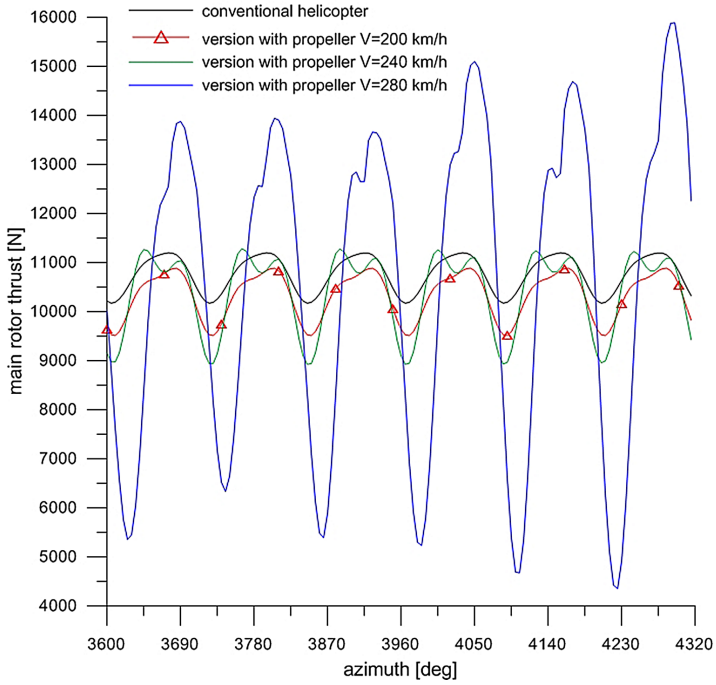

Fig. 27. Changes of the main rotor thrust in the level flight conditions. Comparison for conventional helicopter at speed V=200km/h and version with the propulsive propeller at speed range 200-280km/h; helicopter mass 1,100kg. [Author, 2015]

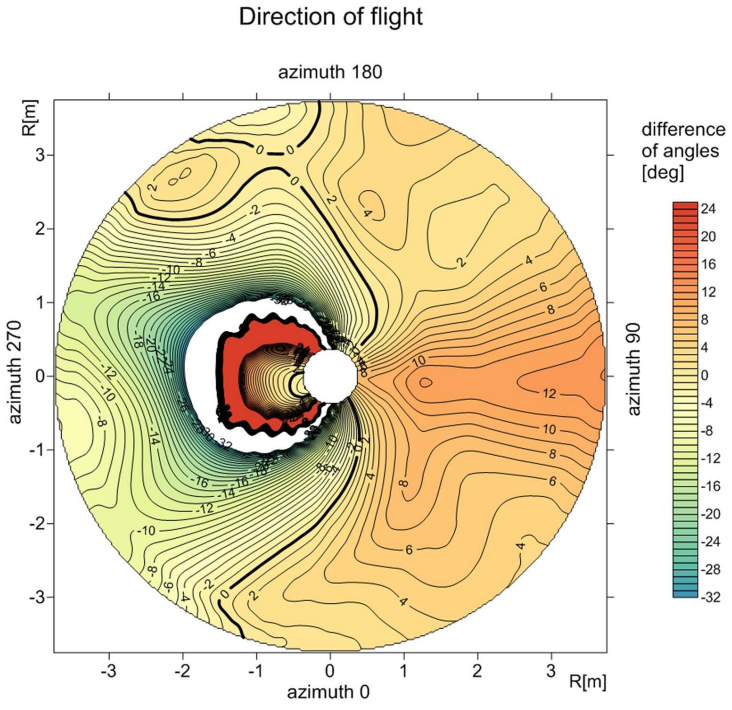

Fig. 28. Main rotor disk distribution of difference of critical and local attack angles of blade cross-sections in level flight at speed 280km/h. The case for the helicopter with propulsive propeller. [Author, 2015]

4. CONCLUSIONS

The results of calculations concerning the influence of applying an additional pushing propeller to the light helicopter indicate that the increment of the maximum flight speed to 230km/h (about 15%) is possible without increasing the power unit and without generating excessive vibrations.

Performing the flights at a small pitch angle of the fuselage to preserve a low value of the helicopter drag coefficient at high speed creates airflow directed, like in an autorotation state, from lower to upper surface of the rotor disk but with the separation zone located at the root and middle sections of the blade.

The enlarging separation zone at blade sections can be the reason of control load increase, but it should be noticed that applying an additional propeller may improve the control of helicopter in the range of a lower flight speed especially in terms of an accelerating and decelerating maneuver without a change of the helicopter pitch angle.

REFERENCES

[1] Hirschberg M. (2010), X2, X3, S-97, and X-49: The Battle of the Compounds is Joined, *Vertiflite*, volume 56, no.4, pages 16-22
[2] Hirschberg M. (2014), Raider Rolls Out, *Vertiflite*, volume 60, no.6, pages 12-13
[3] Gruszczyński J., Fiszer M. (2014), Airbus Helicopters X3. Demonstrator hybrydowego śmigłowca, *Lotnictwo* 10/2014, (in Polish)
[4] Szopa M. (2013), Sikorsky S-97 Raider - przełom w dziedzinie wiropłatów ? , *Lotnictwo* 10/2013, pages 70-73, (in Polish)
[5] Hopkins H. (1986), Fastest blades in the world, *Flight International* , 27 December 1986 , p. 24-27
[6] Wiśniowski W.: (2014), Specjalizacje Instytutu Lotnictwa - Przegląd i wnioski, Prace Instytutu Lotnictwa, no.1(235), Warszawa 2014, pages 7-16, (in Polish)
[7] Wiśniowski W.: (2014), XX lat programu samolotów lekkich i bezpieczeństwa, Prace Instytutu Lotnictwa, no.1(236), Warszawa 2014, pages 7-25, (in Polish)
[8] Stanisławski J.: Obliczenia obciążeń śmigłowca ILX-27, Institute of Aviation, internal report ILX27/0001/BP2/2012, Warszawa 2012, (in Polish).
[9] Stanisławski J.: Porównanie wyników pomiarów oraz symulacji obliczeniowych pracy śmigłowca ILX-27, Institute of Aviation, internal report ILX27/0014/BP2/2013, Warszawa 2013, (in Polish).

STANY LOTU ŚMIGŁOWCA LEKKIEGO Z DODATKOWYM ŚMIGŁEM NAPĘDOWYM

Streszczenie

Przedstawiono możliwości zmian stanów lotu śmigłowca lekkiego poprzez zabudowę śmigła napędowego. Zastosowanie dodatkowego śmigła wpływa na zmniejszenie mocy niezbędnej wirnika nośnego. Porównano wyniki obliczeń stanów lotu z zastosowaniem uproszczonego modelu wirnika dla śmigłowca konwencjonalnego oraz wersji z dodatkowym śmigłem. Do wyznaczenia obciążeń wirnika z uwzględnieniem odkształceń łopat wykorzystano dokładniejszy model obliczeniowy, gdzie równania ruchu elastycznej łopaty wirnika rozwiązywano metodą Runge-Kutta.

Słowa kluczowe: śmigłowiec, śmigło pchające, wirnik.